LETTER

doi:10.1038/nature13856

The power of relativistic jets is larger than the luminosity of their accretion disks

G. Ghisellini[1], F. Tavecchio[1], L. Maraschi[1,2], A. Celotti[1,3,4] & T. Sbarrato[1,5,6]

Theoretical models for the production of relativistic jets from active galactic nuclei predict that jet power arises from the spin and mass of the central supermassive black hole, as well as from the magnetic field near the event horizon[1]. The physical mechanism underlying the contribution from the magnetic field is the torque exerted on the rotating black hole by the field amplified by the accreting material. If the squared magnetic field is proportional to the accretion rate, then there will be a correlation between jet power and accretion luminosity. There is evidence for such a correlation[2–8], but inadequate knowledge of the accretion luminosity of the limited and inhomogeneous samples used prevented a firm conclusion. Here we report an analysis of archival observations of a sample of blazars (quasars whose jets point towards Earth) that overcomes previous limitations. We find a clear correlation between jet power, as measured through the γ-ray luminosity, and accretion luminosity, as measured by the broad emission lines, with the jet power dominating the disk luminosity, in agreement with numerical simulations[9]. This implies that the magnetic field threading the black hole horizon reaches the maximum value sustainable by the accreting matter[10].

The jet power is predicted[1] to depend on $(aMB)^2$, where a and M are respectively the spin and mass of the black hole and B is the magnetic field at its horizon. Seed magnetic fields are amplified by the accretion disk up to equipartition with the mass energy density, $\sim\rho c^2$ (c, speed of light; ρ, density), of the matter accreting at the rate $\dot{M}$. A greater $\dot{M}$ implies a larger ρ, which can sustain a larger magnetic field. This field can in turn tap a larger amount of the black hole rotational energy. The magnetic field is thus a catalyst for the process. Increasing the spin of the black hole shrinks the innermost stable orbit, increasing the accretion efficiency $\eta = L_{\rm disk}/\dot{M}c^2$ ($L_{\rm disk}$, accretion disk luminosity) to a maximum value[11] $\eta = 0.3$.

We use a well-designed sample of blazars that have been detected in the γ-ray wavelength band by the Fermi Large Area Telescope (LAT) and spectroscopically observed in the optical band[12,13] (Methods). They have been classified as BL Lacertae objects or flat-spectrum radio quasars (FSRQs) according to whether the rest-frame equivalent width of their broad emission lines was greater than (FSRQ) or smaller than (BL Lac) 5 Å (rest frame). The sample contains 229 FSRQs and 475 BL Lacs. Of the latter, 209 have a spectroscopically measured redshift. We considered all FSRQs with enough multiwavelength data to have a spectral energy distribution that allows the bolometric luminosity to be established. This amounts to 191 objects. For BL Lacs, we consider only the 26 sources for which broad emission lines were detected. This makes them the low-disk-luminosity tail of the full blazar sample. This choice is dictated by our desire to measure the accretion luminosity, together with the jet power. Through the visible broad emission lines, we reconstruct, using a template[14,15], the luminosity of the entire broad line region ($L_{\rm BLR}$). The latter is a proxy for the accretion disk luminosity, $L_{\rm BLR} = \phi L_{\rm disk}$, with[16] $\phi \approx 0.1$. The accretion disk luminosity is then directly given by the observed broad emission lines, avoiding contamination by the non-thermal continuum. Uncertainties are admittedly large (a factor of ∼2) for specific sources, but the averages should be representative of the true values.

To model the non-thermal jet emission, we applied to all objects a simple, one-zone leptonic model[17] (Methods), from which we derive the physical parameters of the jet. The only parameter of interest here, however, is the bulk Lorentz factor (Γ) of the outflowing plasma, found to lie in the range 10–15 (Methods and Extended Data Fig. 2). This range is similar to that obtained from measurements of the superluminal motion of the radio components, but that occurs at larger distances from the black hole. The bulk Lorentz factor is thus only weakly model dependent. The power that the jet expends in producing the non-thermal radiation is[18]

$$P_{\rm rad} = 2f\frac{L_{\rm jet}^{\rm bol}}{\Gamma^2} \quad (1)$$

where $L_{\rm jet}^{\rm bol}$ is the bolometric jet luminosity, the factor of 2 accounts for the two jets and f is of order unity (Methods). If this were the entire power of the jet, it would be entirely spent in producing the observed radiation. The jet would stop, and could not produce the radio lobes or the extended radio emission we see from these objects. It is thus a strict lower limit to the jet power.

Figure 1 shows $P_{\rm rad}$ as a function of $L_{\rm disk}$ for the 217 blazars that we consider. There is a robust correlation between the two: $\log(P_{\rm rad}) = 0.98\log(L_{\rm disk}) + 0.639$ (with a probability $P < 10^{-8}$ of being random, even taking into account the common redshift dependence). We thus find a linear correlation between the minimum jet power and the accretion luminosity, as expected. Moreover, the two are of the same order. We note that this holds also for the considered BL Lacs that do show broad emission lines. The dispersion along the fitting line is $\sigma = 0.5$ dex. An important contribution to this dispersion comes from the large amplitude variability of the non-thermal flux displayed by all blazars, especially in the γ-ray band, where the bolometric jet luminosity peaks. This is true even if we consider the LAT luminosity averaged over two years[19], as shown by the comparison between LAT and the older Energetic Gamma Ray Experiment Telescope (EGRET, on board the Gamma Ray Compton Observatory) results. About 20% of the EGRET-detected blazars are not detected by LAT[20], even though the sensitivity of the latter is 20-fold higher.

The power in radiation ($P_{\rm rad}$) is believed to be about 10% of the jet power ($P_{\rm jet}$), and, remarkably, this holds both for active galactic nuclei and γ-ray bursts[21]. We confirm this result for the case in which there is one proton per emitting lepton (Methods and Extended Data Fig. 1). This limits the importance of electron–positron pairs, which would reduce the total jet power. In addition, pairs cannot largely outnumber protons, because otherwise the Compton rocket effect would stop the jet[18] (Methods).

An inevitable consequence of $P_{\rm jet} \approx 10P_{\rm rad}$ is that the jet power is larger than the disk luminosity. Therefore, the process that launches and accelerates jets must be extremely efficient, and might be the most efficient way of transporting energy from the vicinity of the black hole to infinity.

[1]Istituto Nazionale di Astrofisica – Osservatorio Astronomico di Brera, Via E. Bianchi 46, I–23807 Merate, Italy. [2]Istituto Nazionale di Astrofisica – Osservatorio Astronomico di Brera, Via E. Brera 28, I–20121 Milano, Italy. [3]Scuola Internazionale Superiore di Studi Avanzati, Via Bonomea 265, I–34135 Trieste, Italy. [4]Istituto Nazionale di Fisica Nucleare – Sezione di Trieste, Via Valerio 2, I-34127 Trieste, Italy. [5]Università dell'Insubria, Dipartimento di Fisica e Matematica, Via Valleggio 11, I–22100 Como, Italy. [6]European Southern Observatory, Karl-Schwarzschild-Strasse 2, 8578 Garching bei München, Germany.

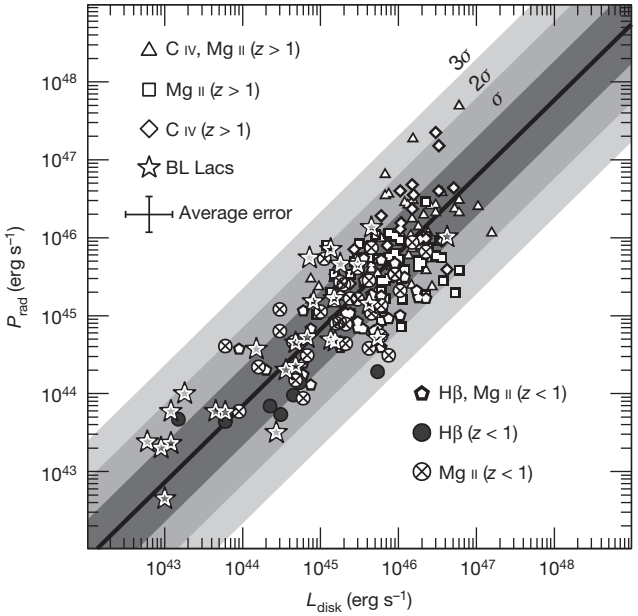

Figure 1 | Radiative jet power versus disk luminosity. The radiative jet power versus the disk luminosity, calculated as ten times the luminosity of the broad line region. Different symbols correspond to the different emission lines used to estimate the disk luminosity, as labelled. All objects were detected using Fermi/LAT and have been spectroscopically observed in the optical[12,13]. Shaded areas correspond to 1σ, 2σ and 3σ (vertical) dispersion, where $\sigma = 0.5$ dex. The black line is the least-squares best fit ($\log(P_{rad}) = 0.98\log(L_{disk}) + 0.639$). The average error bar corresponds to uncertainties of a factor of 2 in L_{disk} (ref. 16) and 1.7 in P_{rad} (corresponding to the uncertainty in Γ^2).

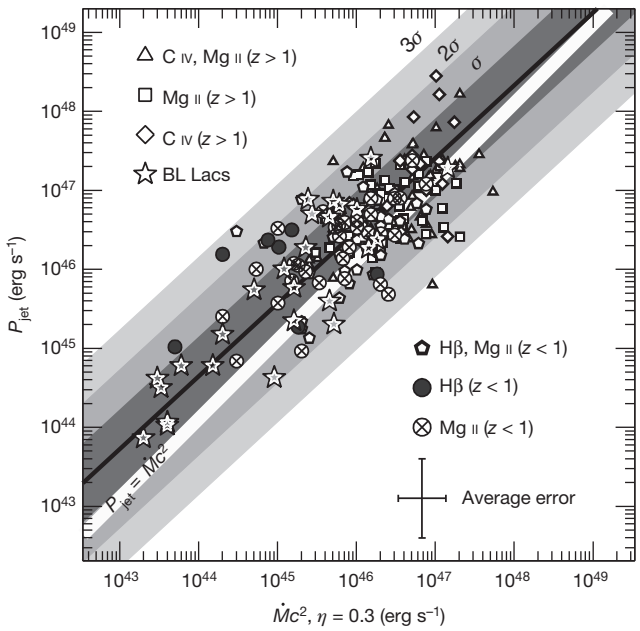

Figure 2 | Jet power versus accretion power. The total jet power estimated using a simple one-zone leptonic model[17], assuming one cold proton per emitting electron, versus $\dot{M}c^2$ calculated assuming an efficiency $\eta = 0.3$, which is appropriate for a maximally rotating Kerr black hole. Different symbols correspond to the different emission lines used to estimate the disk luminosity, as in Fig. 1. Shaded areas correspond to 1σ, 2σ and 3σ (vertical) dispersion, where $\sigma = 0.5$ dex. The black line is the least-squares best fit ($\log(P_{jet}) = 0.92\log(\dot{M}c^2) + 4.09$). The white stripe is the equality line. The average error bar is indicated ($\dot{M}c^2$ has the same average uncertainty of L_{disk}; the average uncertainty in P_{jet} is a factor of 3).

Assuming that $\eta = 0.3$, appropriate for rapidly rotating black holes, we have $\dot{M}c^2 = L_{disk}/\eta$. Figure 2 shows P_{jet} versus $\dot{M}c^2$ for all our sources. The white stripe indicates $P_{jet} = \dot{M}c^2$, and the black line is the best-fit correlation ($\log(P_{jet}) = 0.92\log(\dot{M}c^2) + 4.09$) and always lies above the equality line. This finding is fully consistent with recent general relativistic magnetohydrodynamic numerical simulations[9] in which the average outflowing power in jets and winds reaches 140% of $\dot{M}c^2$ for dimensionless spin values $a = 0.99$. The presence of the jet implies that the gravitational potential energy of the falling matter can not only be transformed into heat and radiation, but can also amplify the magnetic field, allowing the field to access the large store of black hole rotational energy and transform part of it into mechanical power in the jet. This jet power is somewhat larger than the entire gravitational power ($\dot{M}c^2$) of the accreting matter. This is not a coincidence, but is the result of the catalysing effect of the magnetic field amplified by the disk. When the magnetic energy density exceeds the energy density ($\sim\rho c^2$) of the accreting matter in the vicinity of the last stable orbit, the accretion is halted and the magnetic energy decreases, as shown by numerical simulations[9,22] and confirmed by recent observational evidence[10].

The mass of the black holes of the FSRQs in our sample has been calculated[12] assuming that the size of the broad line region scales with the square root of the ionizing disk luminosity as indicated by reverberation mapping[23,24], and by assuming that the clouds producing the broad emission lines are virialized. The uncertainties associated with this method are large (dispersion of $\sigma = 0.5$ dex for the black hole mass values[25]), but if there is no systematic error (Methods) then the average Eddington ratio for FSRQs is reliable: $\langle L_{disk}/L_{Edd}\rangle = 0.1$ (L_{Edd}; Eddington luminosity; Extended Data Fig. 2). This implies that all FSRQs should have standard, geometrically thin, optically thick accretion disks[26]. Therefore, the more powerful jets (the ones associated with FSRQs) can be produced by standard disks with presumably no central funnel, contrary to some expectations[27,28].

A related issue is the possible change of accretion regime at low accretion rate (in Eddington units), or, equivalently, when $L_{disk} \lesssim 10^{-2} L_{Edd}$. In this case, the disk is expected to become radiatively inefficient, hotter and geometrically thick. How the jet responds to such changes is still an open issue. An extension of our study to lower luminosities could provide some hints. Another open issue is how the jet power depends on the black hole spin[29]. Our source sample consists by construction of luminous γ-ray sources that presumably have the most powerful jets, and thus have the most rapidly spinning holes. It will be interesting to explore less luminous jetted sources, to gain insight into the possible dependence of the jet power on the black hole spin and the possible existence of a minimum spin value for the jet to exist. In turn, this should shed light on the longstanding problem of the radio-loud/radio-quiet quasar dichotomy[30].

Online Content Methods, along with any additional Extended Data display items and Source Data, are available in the online version of the paper; references unique to these sections appear only in the online paper.

Received 25 April; accepted 11 September 2014.

1. Blandford, R. D. & Znajek, R. L. Electromagnetic extraction of energy from Kerr black holes. *Mon. Not. R. Astron. Soc.* **179,** 433–456 (1977).
2. Rawlings, S. & Saunders, R. Evidence for a common central-engine mechanism in all extragalactic radio sources. *Nature* **349,** 138–140 (1991).
3. Celotti, A. & Fabian, A. C. The Kinetic power and luminosity of parsec-scale radio jets – an argument for heavy jets. *Mon. Not. R. Astron. Soc.* **264,** 228–236 (1993).
4. Celotti, A., Padovani, P. & Ghisellini, G. Jets and accretion processes in active galactic nuclei: further clues. *Mon. Not. R. Astron. Soc.* **286,** 415–424 (1997).
5. Maraschi, L. & Tavecchio, F. The jet–disk connection and blazar unification. *Astrophys. J.* **593,** 667–675 (2003).
6. Punsly, B. & Tingay, S. J. PKS 1018–42: a powerful, kinetically dominated quasar. *Astrophys. J.* **640,** L21–L24 (2006).
7. Celotti, A. & Ghisellini, G. The power of blazar jets. *Mon. Not. R. Astron. Soc.* **385,** 283–300 (2008).
8. Ghisellini, G. *et al.* General physical properties of bright Fermi blazars. *Mon. Not. R. Astron. Soc.* **402,** 497–518 (2010).
9. Tchekhovskoy, A., Narayan, R. & McKinney, J. C. Efficient generation of jets from magnetically arrested accretion on a rapidly spinning black hole. *Mon. Not. R. Astron. Soc.* **418,** L79–L83 (2011).

10. Zamaninasab, M., Clausen–Brown, E., Savolainen, T. & Tchekhoskoy, A. Dynamically important magnetic fields near accreting supermassive black holes. *Nature* **510,** 126–128 (2014).
11. Thorne, K. Disk–accretion onto a black hole. II. Evolution of the hole. *Astrophys. J.* **191,** 507–519 (1974).
12. Shaw, M. S., Romani, R. W., Cotter, G. *et al.* Spectroscopy of broad–line blazars from 1LAC. *Astrophys. J.* **748,** 49 (2012).
13. Shaw, M. S., Romani, R. W., Cotter, G. *et al.* Spectroscopy of the largest ever γ-ray-selected BL Lac sample. *Astrophys. J.* **764,** 135 (2013).
14. Francis, J. *et al.* A high signal–to–noise ratio composite quasar spectrum. *Astrophys. J.* **373,** 465–470 (1991).
15. Vanden Berk, D. E., Richards, G. T. & Bauer, A. Composite quasar spectra from the Sloan Digital Sky Survey. *Astron. J.* **122,** 549–564 (2001).
16. Calderone, G., Ghisellini, G., Colpi, M. & Dotti, M. Black hole mass estimate for a sample of radio-loud narrow-line Seyfert 1 galaxies. *Mon. Not. R. Astron. Soc.* **431,** 210–239 (2013).
17. Ghisellini, G. & Tavecchio, F. Canonical high–power blazars. *Mon. Not. R. Astron. Soc.* **397,** 985–1002 (2009).
18. Ghisellini, G. & Tavecchio, F. Compton rockets and the minimum power of relativistic jets. *Mon. Not. R. Astron. Soc.* **409,** L79–L83 (2010).
19. Nolan, P. L., Abdo, A. A., Ackermann, M. *et al.* Fermi Large Area Telescope second source catalog. *Astrophys. J. Suppl. Ser.* **199,** 31 (2012).
20. Ghirlanda, G., Ghisellini, G., Tavecchio, F., Foschini, L. & Bonnoli, G. The radio–γ-ray connection in Fermi blazars. *Mon. Not. R. Astron. Soc.* **413,** 852–862 (2011).
21. Nemmen, R. S. *et al.* A universal scaling for the energetics of relativistic jets from black hole systems. *Science* **338,** 1445–1448 (2012).
22. Tchekhovskoy, A., Metzger, B. D., Giannios, D. & Kelley, L. Z. Swift J1644+57 gone MAD: the case for dynamically important magnetic flux threading the black hole in a jetted tidal disruption event. *Mon. Not. R. Astron. Soc.* **437,** 2744–2760 (2014).
23. Peterson, B. M. & Wandel, A. Evidence for supermassive black holes in active galactic nuclei from emission-line reverberation. *Astrophys. J.* **540,** L13–L16 (2000).
24. McLure, R. J. & Dunlop, J. S. The cosmological evolution of quasar black hole masses. *Mon. Not. R. Astron. Soc.* **352,** 1390–1404 (2004).
25. Vestergaard, M. & Peterson, B. M. Determining central black hole masses in distant active galaxies and quasars. II. Improved optical and UV scaling relationships. *Astrophys. J.* **641,** 689–709 (2006).
26. Shakura, N. I. & Sunyaev, R. A. Black holes in binary systems. Observational appearance. *Astron. Astrophys.* **24,** 337–355 (1973).
27. Livio, M., Ogilvie, G. I. & Pringle, J. E. Extracting energy from black holes: the relative importance of the Blandford-Znajek mechanism. *Astrophys. J.* **512,** 100–104 (1999).
28. Meier, D. L. Grand unification of AGN and the accretion and spin paradigms. *New Astron. Rev.* **46,** 247–255 (2002).
29. Tchekhovskoy, A., McKinney, J. C. & Narayan, R. General relativistic modeling of magnetized jets from accreting black holes. *J. Phys. Conf. Ser.* **372,** 012040 (2012).
30. Sikora, M., Stawarz, L. & Lasota, J.-P. Radio loudness of active galactic nuclei: observational facts and theoretical implications. *Astrophys. J.* **658,** 815–828 (2007).

Supplementary Information is available in the online version of the paper.

Acknowledgements F.T. and L.M. acknowledge partial funding through a PRIN–INAF 2011 grant.

Author Contributions G.G. wrote the manuscript and fitted all blazars presented. F.T., L.M., A.C. and T.S. contributed to the discussion of the implications of the results.

Author Information Reprints and permissions information is available at www.nature.com/reprints. The authors declare no competing financial interests. Readers are welcome to comment on the online version of the paper. Correspondence and requests for materials should be addressed to G.G. (gabriele.ghisellini@brera.inaf.it).

METHODS

The sample. Our sample is composed of 229 blazars detected by Fermi/LAT[31,32] for which broad emission lines have been measured[12,13,33]. This sample does not include several bright and well-known blazars with historical spectroscopic classifications in the literature. Of these, we have studied the 217 objects with enough multiwavelength information necessary to apply our model. Within the sample, we have 26 BL Lac objects with measured broad emission lines[13]. Therefore our 'BL Lac' objects, even if fulfilling the classical definition of BL Lacs (emission lines of equivalent width smaller than 5 Å), are not lineless, and can be considered as the low-disk-luminosity tail of the blazar sample.

This is the largest sample of γ-ray-detected sources with measured broad emission lines. From these lines, we can estimate the luminosity $L_{\rm BLR}$ of the entire broad line region (BLR), using standard templates[14,15]. Then we calculate the disk luminosity by assuming that $L_{\rm disk} = 10L_{\rm BLR}$, with an average uncertainty[16] of a factor of 2. Because the lines are isotropically emitted, the estimate of $L_{\rm disk}$ does not depend on the viewing angle. Moreover, $L_{\rm disk}$ estimated from $L_{\rm BLR}$ does not depend on any contamination of non-thermal components. In a few cases (20 out of 217; Supplementary Table 1), the resulting $L_{\rm disk}$ differs by a factor of between 2 and 5 from the value of $L_{\rm disk}$ given by fitting a standard accretion disk, which better fits the optical–ultraviolet data. In these cases, we have chosen the value of $L_{\rm disk}$ given by the disk fitting. From the knowledge of the spectral energy distribution (SED), often dominated by the γ-ray luminosity, we can estimate the bolometric jet luminosity in a reliable way. The knowledge of the disk luminosity and the black hole mass greatly helps to fix two important parameters for the theoretical modelling, making it easier to find a unique solution for the emitting region of the jet that we consider. Although the mass estimate can be affected by a rather large statistical error, there should be no relevant systematic error, because a completely independent method[34,35] led to consistent values.

The bolometric jet luminosity. The SED of blazars is characterized by two broad humps (in the $\nu L(\nu)$-vs-ν representation, where ν is the emission frequency), peaking in the mm–UV and in the MeV–GeV bands. The high-energy bump is often the dominant component, except for low-power (and lineless) BL Lacs[36,37], for which the synchrotron luminosity is more important. This is the reason to select Fermi/LAT-detected blazars: for these objects, we can assess the jet bolometric luminosity with high confidence. However, the amplitude of variability, especially in the γ-ray band, can be larger than 2 orders of magnitude, and even larger if one includes exceptionally high states, such as those experienced by the blazar 3C 454.3 (ref. 38). Taking the mean luminosity over a period of two years averages out short-term variability, but not the secular (>10 yr timescale) one. The γ-ray luminosity measured in detected sources could not represent the average status of the source, but only its high state. However, the γ-ray luminosity correlates with the radio one[20], and a Gaussian distribution of long-term γ-ray variability with $\sigma = 0.5$ dex (that is, a factor of 3), coupled with the Fermi/LAT sensitivity, can fully explain what is observed, including the fact that several strong radio sources are yet undetected in the γ-ray band. As a result, the observed correlations in Figs 1 and 2 could represent jet-active states—rather than the average state—that could correspond to a jet power $P_{\rm jet}$ up to a factor of ∼3 smaller. However, the radio–γ-ray correlation gives us confidence that $P_{\rm jet}$ would still be correlated with $L_{\rm disk}$ and $\dot{M}$. The fact that the process of forming and launching relativistic jets is more powerful than accretion only in jet-active states does not affect the conclusion that this process is indeed more powerful than accretion, even if it does not always works at its maximum pace.

The model used. We summarize here the main features of the model used[39]. It assumes that the jet region emitting most of the non-thermal luminosity is at a distance $R_{\rm diss}$ from the black hole. For this reason, this class of models is called 'one-zone', and they are justified because often (although not always) we see coordinated variability in different frequency bands. The jet is assumed to be conical with semi-aperture angle ψ. We assume that $\psi = 0.1$ (ref. 40), but the exact value is not critical for our results. The emitting region is assumed to be spherical, with radius $R = \psi R_{\rm diss}$, embedded in a homogeneous but tangled magnetic field B. The emitting particles are leptons (requiring less power than the less common alternative of emitting hadrons[41]). The main feature of the model is that it accounts for the radiation fields produced by the emission disk, the broad line region, the dusty torus surrounding the disk, and the re-emitting part of the intercepted radiation in the infrared. The distance of the BLR is assumed to be a function of the disk luminosity, as indicated by recent observations (through the reverberation mapping technique[42]): $R_{\rm BLR} = 10^{17} L_{\rm d,45}^{1/2}$ cm. We assume also that the typical size of the molecular torus scales similarly: $R_{\rm torus} = 2 \times 10^{18} L_{\rm d,45}^{1/2}$ cm (in agreement with very recent reverberation results[43]). Here $L_{\rm d,45}$ is the disk luminosity in units of 10^{45} erg s^{-1}. As a consequence, inside the BLR the radiative energy density corresponding to broad lines is constant: $U_{\rm BLR} \approx 0.1 L_{\rm disk} / 4\pi R_{\rm BLR}^2 c = 1/12\pi$ erg cm^{-3}. A similar expression holds for the energy density of the infrared photons of the torus.

The particle distribution responsible for the produced radiation is derived from a continuity equation assuming continuous injection of relativistic leptons at $R_{\rm diss}$, their radiative cooling, the possible production of electron–positron pairs through photon–photon collisions, and their corresponding radiation. The energy distribution of the injected particles is a broken power law, flat at low energies and steepening above some break energy $\gamma_{\rm b}$. Because the considered emitting region is always compact, its self-absorption frequency is always large, and the model cannot account for the radio flux at observed frequencies smaller than a few hundreds of GHz. These are produced by the superposition of several larger components. The emission produced by the accretion disk is assumed to be a multicoloured black body, with a temperature distribution dictated by the balance of heat production and radiative dissipation[26]. The corresponding values of $L_{\rm disk}$ found through disk fitting are listed in the Supplementary Table 1.

Although the model returns several physical parameters, we concentrate on the ones of interest here: the bulk Lorentz factor Γ and Doppler factor δ, the location of the emitting region and the jet power.

The bulk Lorentz factor and Doppler factor. The bulk Lorentz factor, coupled with the viewing angle $\theta_{\rm v}$, determines the Doppler factor $\delta \equiv 1/[\Gamma(1 - \beta\cos(\theta_{\rm v}))]$. For blazars, we have $\sin(\theta_{\rm v}) \approx 1/\Gamma$ and, thus, $\delta \approx \Gamma$. The following observables are affected by Γ.

(1) The observed $\nu F(\nu)$ flux is amplified by a factor of δ^4 with respect to the co-moving value for the synchrotron (Syn) and the self-Compton (SSC) emission, and more for the flux produced through scattering with photons produced external to the jet[44] (this is because, in the co-moving frame, the external seed photons are not isotropic, but come from the forward direction).

(2) As long as the emitting region is inside the BLR, the corresponding energy density is amplified by a factor of $\sim\Gamma^2$ (independently of $\theta_{\rm v}$). A similar result holds for the infrared emission coming from the torus. If $R_{\rm diss} < R_{\rm BLR}$, the external Compton process probably dominates the SSC process, and the Compton/synchrotron luminosity ratio (equal to the radiative/magnetic energy density ratio in the co-moving frame: $U'_{\rm BLR}/U'_{\rm B}$) becomes proportional to $(\Gamma/B)^2$. The same occurs for the infrared radiation reprocessed by the torus as long as $R_{\rm diss} < R_{\rm torus}$.

(3) The Doppler boosting regulates the importance of the SSC component. In brief, the larger the δ factor, the smaller the synchrotron radiation energy density in the co-moving frame, and, therefore, the smaller the SSC component.

(4) The Doppler factor blueshifts the observed peak frequencies.

In conclusion, several observables depend on combinations of parameters that include the factors Γ and δ. Finding the best representation of the data thus requires finding a preferred value for these parameters.

By modelling the 217 blazars of our sample, we find a rather narrow distribution of the bulk Lorentz factors, peaking at $\Gamma \approx 13$ (Extended Data Fig. 2). A Gaussian fit returns a dispersion of $\sigma = 1.4$. The (few) studied BL Lac objects do not show any difference from FSRQs.

The jet power. The jet carries power in different forms, calculated from

$$P_i = 2\pi R^2 \Gamma^2 c U'_i$$

where the factor of 2 accounts for having two jets, and U'_i is the co-moving energy density of protons (i = p), relativistic electrons (i = e), the magnetic field ($i = B$) and the produced radiation (i = rad). The radiative power $P_{\rm rad}$ can also be found, from[18]

$$P_{\rm rad} = 2\frac{4}{3} L^{\rm obs}_{\rm bol,jet} \frac{\Gamma^2}{\delta^4} \quad \text{(external Compton)}$$

$$P_{\rm rad} = 2\frac{16}{5} L^{\rm obs}_{\rm bol,jet} \frac{\Gamma^4}{\delta^6} \quad \text{(Syn and SSC)}$$

This is the way $P_{\rm rad}$ has been calculated: equation (1) is the approximation for $\delta \approx \Gamma$, and where f corresponds to the numerical factor 4/3 or 16/5.

The main idea is that by applying a radiative model, we derive how much magnetic field and how many emitting leptons are required to account for the observed luminosity, and also the size and the bulk Lorentz factor of the emitting region. We then assume that all leptons present in the jet participate in the emission, and that for each lepton there is a proton. We assume them to be cold, even if shock acceleration, magnetic reconnection or both would give at least equal energy to the leptons and to the protons. This simplification is reasonable as long as the average electron energy remains smaller than the proton rest mass.

The power $P_{\rm rad}$ is a lower limit to the power because if the total jet power were $P_{\rm rad}$ then it would convert all its bulk kinetic energy to produce the radiation we see, and it would stop well before the point at which we see it still moving (using very large-baseline interferometry observations, which sample a region parsecs away from the black hole). The distributions of the different forms of the jet power are shown in the Extended Data Fig. 3, where they are compared with the distribution of $L_{\rm disk}$. To account for $P_{\rm rad}$, the Poynting flux and $P_{\rm e}$ are not sufficient. We need another form of power. The simple solution is to assume that the jet carries enough protons to have $P_{\rm p} > P_{\rm rad}$. This is strengthened by the fact that if the jet were made

up of pairs only, it would suffer a strong deceleration due to the Compton rocket effect when crossing the BLR, and it would stop. In fact, in the co-moving frame of the jet, the external photons are seen coming from the forward direction. Even if the leptons were distributed isotropically, head-on scatterings along the forward direction of the jet axis would be more frequent and energetic than tail-on scatterings. The produced radiation, in the jet co-moving frame, has a forward momentum, compensated by a recoil of the jet emitting region. With no protons, the jet strongly decelerates. To avoid having a strong deceleration[18] (one that halves Γ), the number of pairs should not exceed ~10–20 per proton, in agreement with estimates made with independent methods[7,18,45].

Jet power and location of the emitting region. The location of the emitting region could impact on the required jet power. The emitting region is estimated to be at distances $R_{\rm diss} < R_{\rm BLR}$ (85% of the sources) or at $R_{\rm BLR} < R_{\rm diss} < R_{\rm torus}$ (15% of the sources). This is dictated by the SED properties (that is, if the Compton peak is at ~MeV energies then a seed external field of lower frequency is preferred). Locating the source much further out, where there are no important sources of external photons, would increase the jet power requirements, as shown below. We have the following two possibilities.

First, the SED could result from Syn and SSC. In this case, the parameters can be found unequivocally[46]. The synchrotron ($\nu_{\rm S}$)/Compton ($\nu_{\rm C}$) peak frequency ratio gives $\gamma^2_{\rm peak}$. The Compton dominance (Compton/synchrotron luminosity ratio, $L_{\rm C}/L_{\rm S}$) and the definition of $\nu_{\rm S} = 3.6\times10^6\gamma^2_{\rm peak}\delta/(1+z)$ give

$$B\delta^2 = \frac{L_{\rm syn}}{R}\left[\frac{2}{cL_{\rm C}}\right]^{1/2}$$

$$B\delta = \frac{\nu_{\rm S}^2}{3.6\times10^6\nu_{\rm C}(1+z)}$$

By solving for B and δ (setting $R = ct_{\rm var.}\delta/(1+z)$) and inserting typical values of the observables (that is, $t_{\rm var.}\approx 1$ d, $\nu_{\rm S}\approx 10^{13}$ Hz, $\nu_{\rm C}\approx 10^{22}$ Hz, $L_{\rm S}\approx 10^{46}$ erg s^{-1} and $L_{\rm C}\approx 10^{47}$ erg s^{-1}), we find small B ($\lesssim 10^{-4}$ G) and large δ ($\gtrsim 100$). A large δ in turn requires very small viewing angles ($<1^\circ$, causing problems with determining the number of sources belonging to the parent population) and large Γ. As a consequence, the energy densities inside the source are very small, making the cooling time very long. Invoking second-order SSC emission does not help, because all co-moving radiation energy densities are small, because δ is large. The pure SSC process, applied to the sources in our sample, is thus very inefficient. This implies that more emitting electrons are needed to produce the observed flux, even accounting for the larger beaming. $P_{\rm rad}$ is small (because it is proportional to Γ^{-2}), but $P_{\rm e}$ is increased. The source is not in equipartition, and its total minimum power is greater than it would be if the source were in a dense external photon environment[47]. We have directly tested this by applying the pure SSC model to some sources. In the case of 0325+2224, at $z = 2.066$, we find that $\log(P_{\rm rad}) = 44.9$, $\log(P_{\rm p}) = 48.6$, $\log(P_{\rm e}) = 47.3$ and $\log(P_{\rm B}) = 42.4$, to be compared with the values in Supplementary Table 1. Far from sources of external photons (that is, pure SSC), the required total jet power increases. Having two emitting regions (one for the synchrotron, another for the inverse-Compton components) does not help, because the component emitting the γ-rays must produce less synchrotron radiation than we see, requiring an even smaller magnetic field: the radiative cooling is even less, and the entire process is even less efficient. Because the probability that a single emitting region is aligned with the observer to within 1° (as required by the large δ) is very small, there must be several of these small regions pointing in different directions. The power that we calculate on the basis of observations refers to only one of these regions. The total jet power is bound to be much more.

Second, the SED could result from a spine–layer structure, that is, a slow layer surrounding a fast spine. The layer emits, and its photons are scattered by the spine, enhancing its Compton flux with respect to the pure SSC case. The radiative cooling is then more efficient. This model is very similar to the one we used, with one difference: using the external photons made by the BLR and the torus does not involve loss of jet energy, while using the photons made by the layer implies that the jet puts some energy and power also in the layer, besides in the spine. This model therefore inevitably implies a more powerful jet.

Low-energy electrons and jet power. The energy distribution of injected electrons has a flat slope ($\propto\gamma^{-s_1}$) at low energies, with $-1 < s_1 < 1$. We then calculate the particle distribution $N(\gamma)$ at the time $R_{\rm blob}/c$, and the cooling energy $\gamma_{\rm cool}$ at this time. Electrons of energy $\gamma < \gamma_{\rm cool}$ retain the injected slope. Owing to the flat s_1, the number of electrons between $\gamma\approx 1$ and $\gamma_{\rm cool}$ is small compared with the number of electrons above $\gamma_{\rm cool}$. In the external-Compton scenario, low-energy electrons are responsible for the X-ray spectrum, and so the value of $\gamma_{\rm cool}$ is constrained by the data. The total number of emitting electron is well constrained.

Electron–positron pairs and jet power. If electron–positron pairs are present, the number of protons is reduced, with a corresponding reduction of the jet power, up to a factor of 10 (not to suffer too strong a Compton rocket effect). However, producing the required number of pairs is problematic. In fact they cannot be produced at $R_{\rm diss}$. They would be relativistic from the start and would emit X-rays, filling the 'valley' in the X-ray part of the SED[48]. They cannot be produced by the accretion disk, which is too cold. The only possible source is the initial, accelerating part of the jet, whose observed radiation is overwhelmed by the much more beamed flux produced at $R_{\rm diss}$. This possibility requires a self-absorbing synchrotron flux and quasi-thermal Comptonization causing the spectrum to peak exactly at 1 MeV (ref. 49). A peak at higher energies implies pairs that are relativistic from the start and fewer in number; a peak below the pair-production threshold $m_{\rm e}c^2$ implies too few produced pairs. We find this scenario rather ad hoc and very unlikely to occur in all sources.

Consider also that (1) if $P_{\rm jet}$ is lowered by a factor of 10 then almost half of the sources in our sample would have $P_{\rm jet} < P_{\rm rad}$ (Fig. 1), implying that the jet stops at $R_{\rm diss}$ (and that no radio halo or superluminal motion would be possible); and that (2) it is found that $P_{\rm jet}\approx 10P_{\rm rad}$ for blazars and for γ-ray bursts, using arguments completely different from ours[21].

31. Abdo, A. A. *et al.* The first catalog of active galactic nuclei detected by the Fermi Large Area Telescope. *Astrophys. J.* **715,** 429–457 (2010).
32. Ackermann, M. *et al.* The second catalog of active galactic nuclei detected by the Fermi Large Area Telescope. *Astrophys. J.* **743,** 171 (2011).
33. Shen, Y. *et al.* A catalog of quasar properties from Sloan Digital Sky Survey data release 7. *Astrophys. J. Supp. Ser.* **194,** 45 (2011).
34. Ghisellini, G. Extragalactic relativistic jets. *AIP Conf. Proc.* **1381,** 180–198 (2011).
35. Sbarrato, T. *et al.* Blazar candidates beyond redshift 4 observed with GROND. *Mon. Not. R. Astron. Soc.* **433,** 2182–2193 (2013).
36. Fossati, G., Maraschi, L., Celotti, A., Comastri, A. & Ghisellini, G. A unifying view of the spectral energy distributions of blazars. *Mon. Not. R. Astron. Soc.* **299,** 433–448 (1998).
37. Donato, D., Ghisellini, G., Tagliaferri, G. & Fossati, G. Hard X-ray properties of blazars. *Astron. Astrophys.* **375,** 739–751 (2001).
38. Bonnoli, G., Ghisellini, G., Foschini, L., Tavecchio, F. & Ghirlanda, G. The γ-ray brightest days of the blazar 3C 454.3. *Mon. Not. R. Astron. Soc.* **410,** 368–380 (2011).
39. Ghisellini, G. & Tavecchio, F. Canonical high-power blazars. *Mon. Not. R. Astron. Soc.* **397,** 985–1002 (2009).
40. Nalewajko, K., Begelman, M. C. & Sikora, M. Constraining the location of gamma-ray flares in luminous blazars. *Astrophys. J.* **789,** 161 (2014).
41. Böttcher, M., Reimer, A., Sweeney, K. & Prakash, A. Leptonic and hadronic modeling of Fermi-detected blazars. *Astrophys. J.* **768,** 54 (2013).
42. Bentz, M. C., Peterson, B. M., Pogge, R. W., Vestergaard, M. & Onken, C. A. The radius–luminosity relationship for active galactic nuclei: the effect of host–galaxy starlight on luminosity measurements. *Astrophys. J.* **644,** 133–142 (2006).
43. Koshida, S., Minezaki, T., Yoshii, Y. *et al.* Reverberation measurements of the inner radius of the dust torus in 17 Seyfert galaxies. *Astrophys. J.* **788,** 159 (2014).
44. Dermer, C. On the beaming statistics of γ-ray sources. *Astrophys. J.* **446,** L63–L66 (1995).
45. Sikora, M. & Madejski, G. On pair content and variability of subparsec jets in quasars. *Astrophys. J.* **534,** 109–113 (2000).
46. Tavecchio, F., Maraschi, L. & Ghisellini, G. Constraints on the physical parameters of TeV blazars. *Astrophys. J.* **509,** 608–619 (1998).
47. Ghisellini, G. & Celotti, A. Relativistic large-scale jets and minimum power requirements. *Mon. Not. R. Astron. Soc.* **327,** 739–743 (2001).
48. Ghisellini, G. & Madau, P. On the origin of the γ-ray emission in blazars. *Mon. Not. R. Astron. Soc.* **280,** 67–76 (1996).
49. Ghisellini, G. Electron-positron pairs in blazar jets and γ-ray loud radio galaxies. *Mon. Not. R. Astron. Soc.* **424,** L26–L30 (2012).

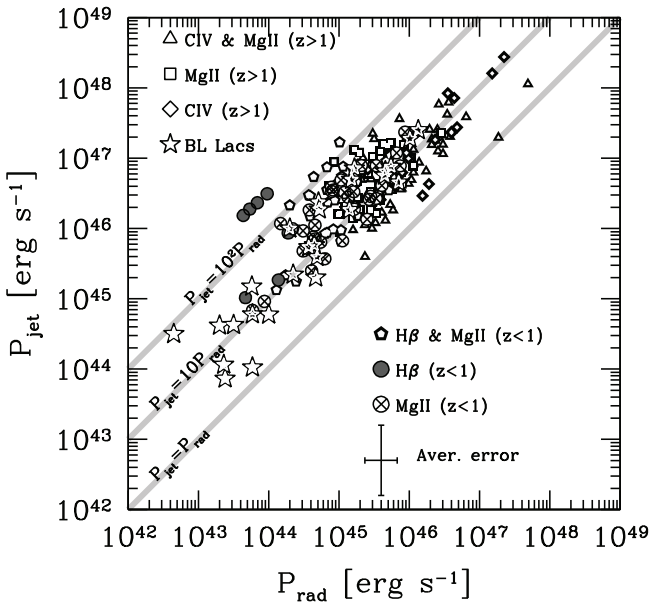

Extended Data Figure 1 | Jet power versus radiative jet power. We compare the total jet power and the radiative jet power for the blazars in our sample. The grey lines, as labelled, respectively correspond to equality and to $P_{\rm jet}$ equal to 10-fold and 100-fold $P_{\rm rad}$. Same symbols as in Fig. 1. The average error bar is indicated.

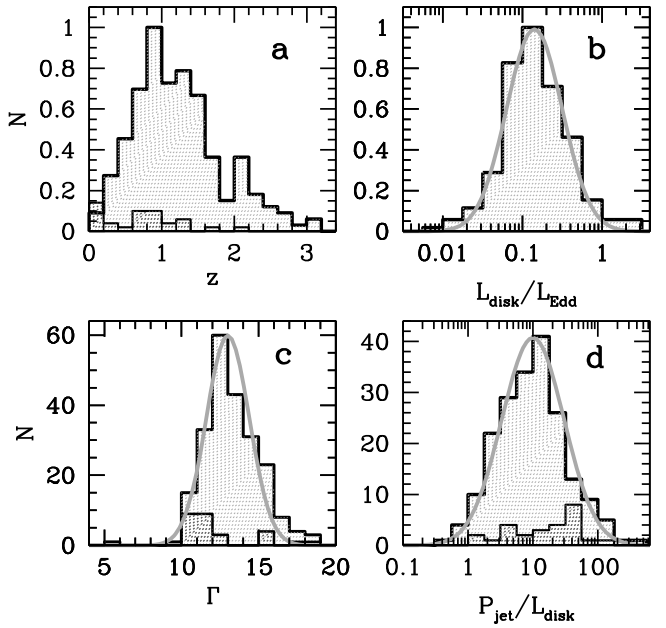

Extended Data Figure 2 | Distribution of relevant quantities. **a**, Normalized redshift distribution for FSRQs (light hatching) and BL Lacs (heavy hatching) in our sample. **b**, Normalized distribution of the ratio $\log(L_{disk}/L_{Edd})$ for FSRQs in our sample. The black hole mass is the virial mass, calculated on the basis of the width of the broad lines[12], compared with a log-normal distribution having a width of $\sigma = 0.35$ dex. **c**, Distribution of the bulk Lorentz factor. Hatching as in **a**. The plotted normal distribution has a width of $\sigma = 1.4$. **d**, Distribution of the ratio $\log(P_{jet}/L_{disk})$ for our sources, including BL Lacs (hatching as in **a**). The shown log-normal distribution has a width of $\sigma = 0.48$ dex.

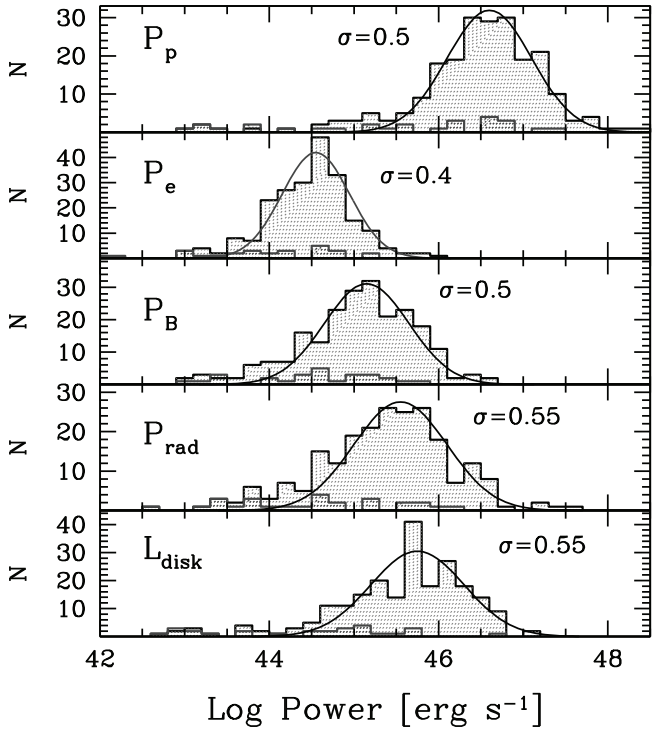

Extended Data Figure 3 | Distribution of jet powers. Jet power distribution for FSRQs (light hatching) and BL Lacs (heavy hatching) in our sample, compared with the disk luminosity distribution as labelled: P_p is the kinetic power of the (cold) protons, assuming one proton per emitting electron; P_e is the power in relativistic emitting electrons; P_B is the jet Poynting flux; P_{rad} is the power that the jet has spent in producing the observed radiation; L_{disk} is the luminosity of the accretion disk. All distributions are fitted with a log-normal distribution. The corresponding value of σ (in dex) is reported. The average values of the distributions are $\langle \log(L_{disk}) \rangle = 45.5$, $\langle \log(P_{rad}) \rangle = 45.3$, $\langle \log(P_B) \rangle = 45.0$, $\langle \log(P_e) \rangle = 44.4$, $\langle \log(P_p) \rangle = 46.4$ (units of luminosity and power are erg s^{-1}).